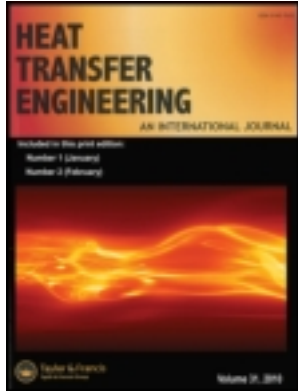


This article was downloaded by: [DTU Library]

On: 10 March 2013, At: 04:28

Publisher: Taylor & Francis

Informa Ltd Registered in England and Wales Registered Number: 1072954 Registered office: Mortimer House, 37-41 Mortimer Street, London W1T 3JH, UK



Heat Transfer Engineering

Publication details, including instructions for authors and subscription information:

<http://www.tandfonline.com/loi/uhte20>

Numerical Analysis of Jet Impingement Heat Transfer at High Jet Reynolds Number and Large Temperature Difference

Michael V. Jensen^a & Jens H. Walther^a

^a Department of Mechanical Engineering, Technical University of Denmark, Kgs. Lyngby, Denmark

Accepted author version posted online: 12 Nov 2012. Version of record first published: 07 Feb 2013.

To cite this article: Michael V. Jensen & Jens H. Walther (2013): Numerical Analysis of Jet Impingement Heat Transfer at High Jet Reynolds Number and Large Temperature Difference, Heat Transfer Engineering, 34:10, 801-809

To link to this article: <http://dx.doi.org/10.1080/01457632.2012.746153>

PLEASE SCROLL DOWN FOR ARTICLE

Full terms and conditions of use: <http://www.tandfonline.com/page/terms-and-conditions>

This article may be used for research, teaching, and private study purposes. Any substantial or systematic reproduction, redistribution, reselling, loan, sub-licensing, systematic supply, or distribution in any form to anyone is expressly forbidden.

The publisher does not give any warranty express or implied or make any representation that the contents will be complete or accurate or up to date. The accuracy of any instructions, formulae, and drug doses should be independently verified with primary sources. The publisher shall not be liable for any loss, actions, claims, proceedings, demand, or costs or damages whatsoever or howsoever caused arising directly or indirectly in connection with or arising out of the use of this material.

Numerical Analysis of Jet Impingement Heat Transfer at High Jet Reynolds Number and Large Temperature Difference

MICHAEL V. JENSEN and JENS H. WALTHER

Department of Mechanical Engineering, Technical University of Denmark, Kgs. Lyngby, Denmark

Jet impingement heat transfer from a round gas jet to a flat wall was investigated numerically for a ratio of 2 between the jet inlet to wall distance and the jet inlet diameter. The influence of turbulence intensity at the jet inlet and choice of turbulence model on the wall heat transfer was investigated at a jet Reynolds number of 1.66×10^5 and a temperature difference between jet inlet and wall of 1600 K. The focus was on the convective heat transfer contribution as thermal radiation was not included in the investigation. A considerable influence of the turbulence intensity at the jet inlet was observed in the stagnation region, where the wall heat flux increased by a factor of almost 3 when increasing the turbulence intensity from 1.5% to 10%. The choice of turbulence model also influenced the heat transfer predictions significantly, especially in the stagnation region, where differences of up to about 100% were observed. Furthermore, the variation in stagnation point heat transfer was examined for jet Reynolds numbers in the range from 1.10×10^5 to 6.64×10^5 . Based on the investigations, a correlation is suggested between the stagnation point Nusselt number, the jet Reynolds number, and the turbulence intensity at the jet inlet for impinging jet flows at high jet Reynolds numbers.

INTRODUCTION

Jet impingement flows provide one of the most efficient ways to transfer energy by convection between a gas and a wall when phase change is not employed. Therefore, jet impingement heating and cooling have found widespread use in industrial applications such as material processing and in the manufacturing industry [1]. Jet impingement heat transfer has been investigated intensively over the last four decades, both experimentally and numerically. Reviews describing the flow physics and proposed heat transfer correlations can be found in references [2] and [3]. They treat both round jet and slot jet configurations. Additionally, reference [3] also includes flame jet impingement heat transfer. Although jet impingement heat transfer has been intensively investigated, most researchers have been focused on jet impingement studies with relatively low to moderate jet Reynolds numbers, generally below 10^5 . These

This work was financially supported by MAN Diesel & Turbo SE and the Danish Center for Applied Mathematics and Mechanics (DCAMM).

Address correspondence to Dr. Jens H. Walther, Department of Mechanical Engineering, Technical University of Denmark, Nils Koppels Allé, Building 403, Kgs. Lyngby DK-2800, Denmark. E-mail: jhw@mek.dtu.dk

studies also focused almost exclusively on impingement flows with a relatively small temperature difference between jet and wall, as also pointed out in reference [4], and thereby a small variation in temperature and density across the wall boundary layer and in the thermophysical gas properties.

The work presented in this article is different from these previous works on jet impingement heat transfer by focusing on jet impingement heat transfer at high jet Reynolds numbers and a large temperature variation across the wall boundary layer in a high-pressure environment. The motivation for the work was an interest in investigating the heat transfer from combustion gasses to the piston surface in large marine diesel engines during the combustion phase of the engine cycle.

In the present work a hot round turbulent gas jet impinging normally onto a colder flat wall was studied numerically at a high jet Reynolds number and a large temperature difference between jet and wall using the commercial computational fluid dynamics (CFD) code STAR-CD version 4.14. The study focused on the convective heat transfer contribution as thermal radiation was not included in the numerical investigation.

The local heat flux distribution along the wall was obtained as the main parameter of interest. The heat flux distribution

was examined for different turbulence intensities at the jet inlet, and the influence on the distribution of applying three different turbulence models was also studied. Furthermore, the influence of the jet Reynolds number and the turbulence intensity at the jet inlet on the stagnation point heat transfer was investigated. Based on this, a correlation is suggested between the stagnation point Nusselt number, the jet Reynolds number, and the turbulence intensity at the jet inlet.

PROBLEM DESCRIPTION

The impinging jet configuration investigated in this study is shown in Figure 1. The impinging jet flow can be divided into three characteristic regions [2]: the free jet region, the stagnation region, and the wall jet region. The jet first develops as a free jet in the free jet region, where momentum transfer with the surrounding gas broadens the jet while decreasing the average jet axial velocity. The jet then enters the stagnation region, where it is decelerated in the direction normal to the wall due to the presence of the wall and is turned into an accelerating flow parallel to the wall. The jet then transforms into a decelerating wall jet in the wall jet region due to momentum transfer across its outer boundary to the surrounding gas and due to momentum exchange with the wall. The radial nature of the flow also contributes to the deceleration of the wall jet. In the free jet region the potential core of the jet extends up to about five jet inlet diameters (D) from the inlet [5]. While almost constant within the potential core, the turbulence intensity increases after the core region due to the mixing of surrounding gas into the jet, and the axial velocity decreases. The increase in turbulence intensity increases the wall heat transfer in the stagnation region for configurations where the distance between the jet inlet and the wall (H) exceeds the length of the potential core as has been observed experimentally [5, 6]. Continuing the increase in distance between the jet inlet and the wall will lead to a decrease in wall heat transfer again. Additionally, the heat transfer distribution along the wall decreases monotonically if the H/D ratio is large, and it typically shows a nonmonotonic behavior with a secondary peak if the H/D ratio is low. The transition is about $H/D = 5$ and associated with the potential core length.

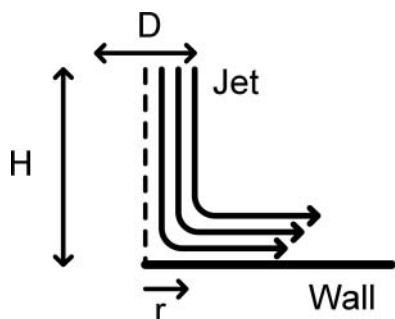


Figure 1 Impinging jet configuration.

The dimensions of the system investigated in this work as well as the thermophysical conditions were chosen based on relevant dimensions and conditions in the combustion chamber of a large marine diesel engine during combustion. The jet inlet diameter D was 0.05 m, and the distance between the jet inlet and the wall H was 0.10 m, resulting in an H/D ratio of 2. The jet temperature at the inlet (T_j) was 2273 K, while the wall temperature (T_w) was 673 K. The jet velocity at the inlet (V) was 10 m/s, and the pressure in the system (p) was 180×10^5 Pa. Both the jet and the surrounding fluid were air. These conditions resulted in a jet Reynolds number (Re) of 1.66×10^5 , where $Re = \rho VD/\mu$ with the density (ρ) and the viscosity (μ) evaluated at the jet temperature at the inlet (T_j).

NUMERICAL MODEL

The numerical study of the impinging jet problem with the dimensions and conditions stated in the previous section was carried out using the commercial CFD code STAR-CD version 4.14. The STAR-CD code employs the finite volume method and a discretization up to second order of the governing Navier–Stokes equations, mass, energy and turbulence equations. Details on the numerical study are given in the following.

Geometry and Boundary Conditions

The impinging round jet configuration was simulated assuming an axisymmetric flow. The dimensions of the computational domain were $2D \times 6D$ in the vertical and horizontal directions, respectively. The geometry is shown in Figure 2. All simulations were performed on a cylindrical structured mesh with gradually refined cells in the wall normal direction close to the wall. In the azimuthal direction the grid consisted of only one cell due to the axisymmetric assumption of the configuration investigated. At the jet inlet an inlet boundary condition was imposed with a plug flow into the domain of 10 m/s and a temperature of 2273 K. The plug flow profile was based on a simplification of

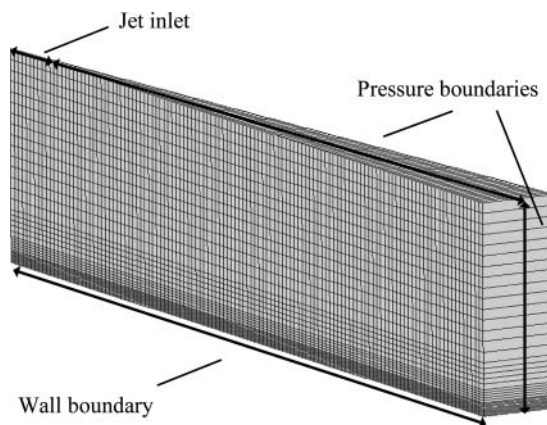


Figure 2 Computational mesh.

the turbulent profile of a jet of combustion products impinging on the piston surface in large marine diesel engines during combustion. The turbulence intensity at the inlet was specified to 5%. The turbulence length scale at the inlet was set to 7% of the jet inlet diameter. A no-slip wall boundary condition with a fixed temperature of 673 K was imposed on the bottom of the domain. At the right (outer) face of the domain and on the top of the domain pressure boundary conditions were imposed with a static pressure of 180×10^5 Pa. At the upper pressure boundary the temperature of the incoming flow was fixed to 2273 K, which equaled the jet temperature at the inlet. On each side of the domain symmetry boundary conditions were imposed to enforce an axisymmetric flow. The assumption of axis symmetry is customary for round jet impingement configurations where the jet impinges normally onto a surface [7–9]. Further investigation of any three-dimensional effects on the flow field in the present configuration was not performed. The mentioned values for temperatures, velocity, pressure, turbulence intensity, and length scale were used in the numerical model for the investigations presented later unless otherwise stated.

Governing Equations

The governing equations are the steady-state Reynolds-averaged Navier–Stokes (RANS) equations:

$$\rho \left(u_j \frac{\partial u_i}{\partial x_j} \right) = -\frac{\partial p}{\partial x_i} + \frac{\partial}{\partial x_j} (\tau_{ij}) \quad (1a)$$

$$\tau_{ij} = \mu \left(\frac{\partial u_i}{\partial x_j} + \frac{\partial u_j}{\partial x_i} \right) - \frac{2}{3} \mu \delta_{ij} \frac{\partial u_k}{\partial x_k} - \overline{\rho u_i' u_j'} \quad (1b)$$

and continuity equation:

$$\frac{\partial}{\partial x_j} (\rho u_j) = 0 \quad (2)$$

and energy equation:

$$\rho \left(u_j \frac{\partial h}{\partial x_j} \right) = \frac{\partial}{\partial x_j} \left(\lambda \frac{\partial T}{\partial x_j} - \overline{\rho u_j' h'} \right) + u_j \frac{\partial p}{\partial x_j} + \tau_{ij} \frac{\partial u_i}{\partial x_j} \quad (3)$$

The governing equations are formulated using the Einstein notation, and δ_{ij} is the Kronecker delta, u_i is the velocity component along the i th coordinate (x_i) direction, and h is the enthalpy. The prime denotes turbulent fluctuations and the overbar time-averaged values of the fluctuation products. Variables without the prime represent time-averaged values, while turbulent fluctuations in density (ρ), dynamic viscosity (μ), and thermal conductivity (λ) were neglected. The density, dynamic viscosity, and thermal conductivity were assumed temperature dependent but independent of pressure, as the pressure variation in the impinging jet flow was small. The maximum Mach number in the flow was 0.01, and the incompressible treatment of the flow was therefore acceptable. As indicated by the momentum equation, Eq. (1), buoyancy effects were neglected. Simulations were also

performed with buoyancy forces included in the flow calculations. These calculations, however, showed negligible influence of the buoyancy effects on the wall heat transfer due to the high fluid momentum in the flow.

Turbulence Modeling

For modeling of turbulence the V2F model [10] was used, which is a RANS type eddy viscosity model. A RANS type eddy viscosity model was selected for two reasons: first, because they are less computationally expensive than more advanced models such as Reynolds stress models (RSM) and large eddy simulation (LES) models; and second, because the aim of the study was to investigate the time-averaged heat transfer in an impinging jet configuration, so instantaneous fluctuating values were not important to resolve. The V2F model does not employ wall functions, so it was necessary with a full resolution of the wall boundary layer (as indicated in Figure 2). The V2F turbulence model has been shown to be one of the most successful RANS type models for predicting heat transfer in jet impingement configurations, especially in the stagnation region, where many other RANS type models are known to fail [1, 8, 9, 11].

Calculations with other turbulence models were also performed. The models were a low-Re k - ϵ model [12] and a k - ϵ RNG model [13] (based on renormalization group theory) employing wall functions to model the viscous sublayer of the flow.

Thermophysical Properties and Density

Temperature-dependent thermophysical properties and density were employed in the numerical model due to the large temperature difference of 1600 K in the investigated configuration. The properties were thermal conductivity (λ), specific heat capacity at constant pressure (c_p), and dynamic viscosity (μ). Polynomial expressions for the temperature dependency were derived based on real gas properties for air [14].

Convergence and Discretization

A global residual tolerance of 10^{-7} was generally needed to ensure convergence of the mass, momentum, and heat transfer computations, which typically resulted in more than 50,000 iterations before convergence was obtained. The heat flux distribution on the wall was monitored to decide whether convergence in the computations was reached. The large number of iterations required to obtain convergence may be due to the application of pressure boundary conditions on large parts of the domain surface and due to the presence of very small cells near the wall in order to resolve the wall boundary layer. The second-order central difference scheme was applied for the discretization of the governing momentum, mass, energy, and turbulence equations in the numerical model. This may also have contributed

to the need for a large number of iterations before convergence was reached.

RESULTS AND DISCUSSION

Results for the heat flux distribution along the wall are presented in terms of the Nusselt number (Nu) distribution. The Nusselt number is calculated as $Nu = \alpha D/\lambda$, where the heat transfer coefficient α is determined as $\alpha = q_w/(T_j - T_w)$ with q_w being the wall heat flux. λ is evaluated at the jet temperature at the inlet (T_j), consistent with the reference temperature used in the evaluation of the jet Reynolds number.

Validation

A direct validation of the numerical model was not possible as no data obtained in a configuration approximating that of the model were found. Instead, predictions obtained with a modified version of the model were compared to experimental heat transfer data of Baughn and Shimizu [6]. In the jet impingement configuration of Baughn and Shimizu, a round air jet issuing from a pipe of 72 pipe diameters impinged normally onto a heated flat plate. The jet Reynolds number in the experiment was 23,750, and the investigated H/D ratios were 2, 6, 10, and 14 (only results for $H/D = 2$ are considered here). The experiment was performed at atmospheric pressure, and the jet temperature at the pipe exit equaled the ambient air temperature. The numerical model was modified to closely approximate the configuration of Baughn and Shimizu in order to avoid differences in the results caused by differences in the configurations. The domain was extended to start two pipe diameters upstream of the pipe exit and hence included a piece of the pipe wall. In radial direction the domain was extended to 10 pipe diameters. A fully developed pipe flow profile, obtained in a separate pipe flow calculation, was imposed as the inlet condition. A constant heat flux was imposed on the wall, the pressure in the domain was 10^5 Pa, and the temperature at the inlet was 293 K, equaling the ambient temperature. Due to only small temperature variations in the domain, the thermophysical properties were assumed constant (evaluated at 293 K), and the ideal gas law was applied for density evaluation.

The obtained Nusselt number distribution is presented in Figure 3 together with the data of Baughn and Shimizu [6]. In the figure are also included distributions obtained with the two other turbulence models mentioned previously, which are described in reference [15]: a low-Re $k-\epsilon$ model [12] and a $k-\epsilon$ RNG model [13] applying standard wall functions (WF) [16]. Computations with different turbulence models were performed, as impinging jets in general are a difficult class of flows to handle for turbulence models in CFD computations, and hence it was relevant to observe the influence of the models on the heat transfer prediction. The low-Re $k-\epsilon$ model required a resolved wall boundary layer like the V2F model, whereas the $k-\epsilon$ RNG model was

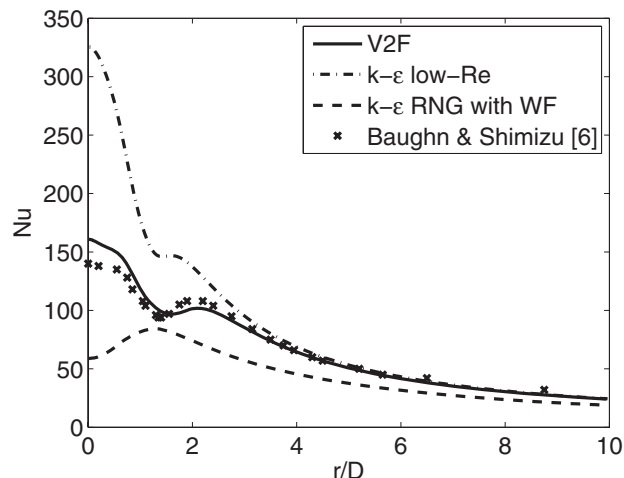


Figure 3 Model predictions versus experimental data [6] for $Re = 23,750$ and $H/D = 2$.

less computationally demanding due to the application of wall functions and hence was applied on a coarser grid.

The Nusselt number distribution predicted by the numerical model applying the V2F turbulence model was in very good agreement with the experimental data. This is in accordance with previous findings in the literature as mentioned earlier. However, the model overpredicted the Nusselt number in the stagnation region, where the maximum deviation between numerical and experimental data was 15%. The Nusselt number distributions obtained when applying the low-Re $k-\epsilon$ and $k-\epsilon$ RNG models were in poor agreement with the experimental results in the stagnation region. The low-Re $k-\epsilon$ model overpredicted the stagnation point Nusselt number by 133%, and the Nusselt number distribution predicted by the $k-\epsilon$ RNG model directly showed a wrong tendency in the stagnation region (the maximum deviation was -58%).

Based on the results in Figure 3, predictions obtained in the validation study applying the V2F turbulence model were considered reasonable. This was taken as an indication of that the numerical model described in the Numerical Model section would produce reliable results. All results presented in the following were obtained with the model described in the “Numerical Model” section.

Grid Independency

To examine grid independency in the numerical calculations of the investigated jet impingement configuration, computations were performed on three consecutively refined grids with 600×38 cells, 1200×90 cells, and 2400×180 cells in the horizontal and vertical directions, respectively. No grid refinement was performed in the azimuthal direction due to the axisymmetric assumption in the calculations. The obtained Nusselt number distributions are shown in Figure 4. The maximum difference between the Nusselt number distributions obtained with the coarsest grid (600×38 cells) and the finest grid (2400×180 cells)

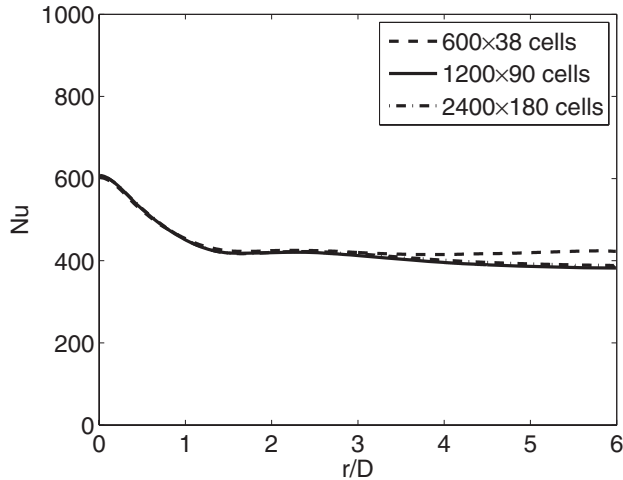


Figure 4 Nusselt number distributions obtained with three consecutively refined grids.

was 9.1%, while the maximum difference was 1.7% between the distributions obtained with the medium refined grid (1200×90 cells) and the finest grid. In the stagnation region, which was of main interest in this work, the three curves nearly coincided with a difference in the distributions of less than 1.1%. Based on these results, the grid consisting of 1200×90 cells was considered to provide sufficient resolution of the computational domain for our investigations. This grid was used in all investigations reported in the following unless otherwise stated. The highest value of the dimensionless wall distance $y^+ = y\sqrt{\tau_w\rho}/\mu$ of the near wall cells using this grid was 0.12; τ_w denotes the wall shear stress, and y is the distance to the wall.

Influence of Domain Size

Nusselt number distributions obtained with grids of different radial extent are shown in Figure 5. Three cases were investigated, where the radial domain extent was 4D, 6D, and 10D, respectively. The cell density in all three grids was the same. Hence, the grid resolution in the case of a radial domain extent of 4D, 6D, and 10D was 800×90 , 1200×90 , and 2000×90 , respectively. The deviation in the heat transfer predictions obtained with the grids having a radial extent of 6D and 10D was small: less than 1.5% for all radial positions. The largest deviation in the heat transfer predictions obtained with the grids having a radial extent of 4D and 10D was 4.9%. In the stagnation region, however, all three Nusselt number distributions nearly coincided. Based on this study, the grid with a radial extent of 6D was regarded to be sufficient for our purpose. It has previously been reported that for domain sizes larger than $8D + H/D$ in the horizontal direction there was no noticeable influence on the flow field and local heat transfer results [11].

Influence of Turbulence Intensity

The influence of the turbulence intensity at the jet inlet (TI) on the wall heat transfer was investigated by varying the turbu-

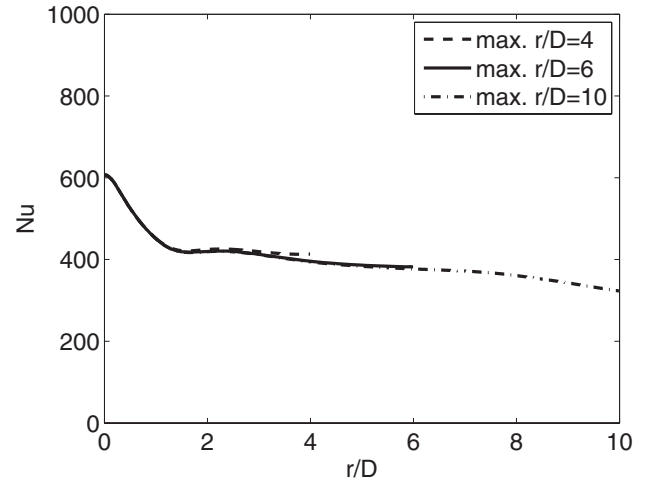


Figure 5 Nusselt number distributions obtained with grids of different radial extent.

lence intensity at the jet inlet boundary from 1.5% to 10%, see Figure 6. It was observed that the turbulence intensity at the jet inlet had a significant influence on the wall heat transfer. The maximum Nusselt number was 387 for a turbulence intensity of $TI = 1.5\%$, while it was 932 for $TI = 10\%$. A secondary peak in the Nusselt number distribution was clearly observed at $r/D = 2.4$ for low turbulence intensities, that is, for $TI = 1.5\%$ and $TI = 2.5\%$. For $TI = 5\%$, a secondary peak was also observed although it was weak. In the case of $TI = 1.5\%$, the maximum Nusselt number occurred at the secondary peak, whereas for the other cases it was located at the stagnation point. For $TI = 10\%$, the Nusselt number values decreased monotonically from the stagnation point without any visible secondary peak. The appearance of a secondary peak in the Nusselt number distribution has been reported in previous experimental works [6, 17, 18], where the location of the peak ranged from $r/D = 2.0$ to $r/D = 2.25$, possibly due to different Reynolds numbers. The secondary peak is believed to be caused by a transition from a laminar to a turbulent boundary layer flow [9, 19] or an

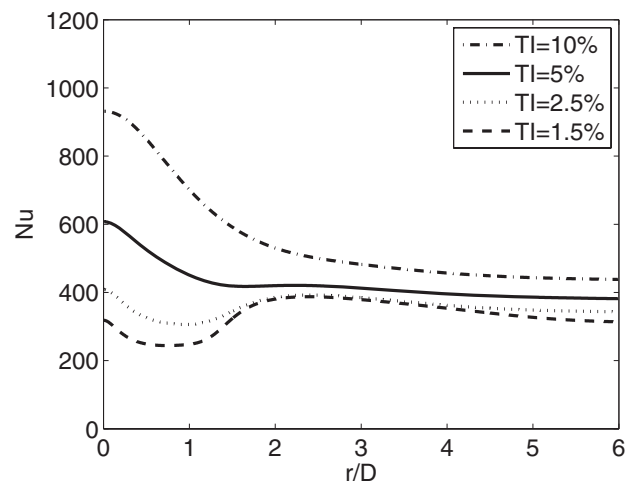


Figure 6 Nusselt number distributions obtained for varying degrees of turbulence intensity at the jet inlet.

augmentation of turbulence kinetic energy due to high shear in the region of streamline convergence [7, 11].

The strong influence of the turbulence intensity at the jet inlet on the wall heat transfer emphasizes the importance of knowing this parameter when comparing different experimental measurements or when comparing with numerical results, as was also pointed out in reference [7].

Influence of Turbulence Model

Computations with the numerical model applying the previously mentioned low-Re $k-\varepsilon$ and $k-\varepsilon$ RNG turbulence models were performed to study the influence on the heat transfer prediction in the investigated configuration. The low-Re $k-\varepsilon$ model was applied on the same grid as that used for the V2F turbulence model (1200×90 cells). The $k-\varepsilon$ RNG model with wall functions was applied on a much coarser grid consisting of 120×35 cells in the horizontal and vertical directions, respectively, without a full resolution of the wall boundary layer. Therefore, in the case of the $k-\varepsilon$ RNG model, y^+ values of the near wall cells were between 38 and 77. The computation times showed that the calculations using the $k-\varepsilon$ RNG model obtained convergence two orders of magnitude faster than the calculations using the other models. The obtained heat transfer results are presented in Figure 7.

A large variation in the predicted wall heat transfer was observed, in both magnitude and trend, when applying the different turbulence models, as was also found in both magnitudes and trends, as was also found in the validation study. The Nusselt number predictions obtained using the V2F model were first decaying until $r/D = 1.6$, whereafter a local maximum was seen at $r/D = 2.2$. The global maximum was at the stagnation point. In the cases of the two other models, the Nusselt number predictions showed a minimum at the stagnation point, and the global maximum was at $r/D = 0.5$ and $r/D = 1.6$, respectively,

in contrast to the V2F predictions. The magnitude of the Nusselt number differed also greatly between the different model predictions, especially in the stagnation region. Most pronounced were the low-Re $k-\varepsilon$ model predictions, which in the stagnation point resulted in a Nusselt number of 1181. This is 94% higher than the V2F model prediction of $Nu = 608$ in the stagnation point. Also the Nusselt number prediction in the stagnation point obtained with the $k-\varepsilon$ RNG model, $Nu = 279$, deviated significantly from the V2F model result by -54% .

In summary, the results in Figure 7 emphasize the problem of handling impinging jet flows for the turbulence models, especially in the stagnation region, which was also observed in the validation study. Except for the tendency in the stagnation region Nusselt number distribution predicted with the low-Re $k-\varepsilon$ model, the tendencies in the different Nusselt number distributions shown in Figure 7 are in general similar to those observed in Figure 3. Therefore, of the three turbulence models examined in the present work, the V2F model is considered to provide the most accurate predictions for the investigated jet impingement case.

Stagnation Point Heat Transfer

Wall heat flux distributions were obtained for different variations of the jet velocity at the inlet and the pressure in the numerical model. One parameter was varied at a time, while the other was kept at the reference value stated in the model description section. The velocities were 10 m/s, 20 m/s, and 40 m/s, and the pressures were 120×10^5 Pa, 150×10^5 Pa, and 180×10^5 Pa. This led to jet Reynolds numbers in the range from 1.10×10^5 to 6.64×10^5 . The calculations were performed with a turbulence intensity at the jet inlet of 5%. Additional calculations were performed with turbulence intensities at the jet inlet of 1.5%, 2.5%, and 10% at some of the jet Reynolds numbers in order to study the influence on the stagnation point heat transfer. The corresponding stagnation point Nusselt numbers (Nu_0) are plotted against the jet Reynolds numbers in Figure 8.

In the case of a fixed turbulence intensity at the jet inlet, the relationship between the stagnation point Nusselt number and the jet Reynolds number can be approximated by a correlation of the form $Nu_0 = CRe^\gamma$, where γ and C are constants, that is, a linear relationship on the log-log plot in Figure 8. However, for different values of the turbulence intensity at the jet inlet, γ and C vary. Therefore, γ and C should be functions of TI. In the cases of $TI = 1.5\%$, 2.5% , 5% , and 10% , the exponent γ was found to be 0.79, 0.84, 0.96, and 1.10, respectively. The form of the correlation between Nu_0 and Re is similar to that previously found in both experimental and numerical works on jet impingement heat transfer [11, 19, 20]. However, the exponent value, ranging from 0.79 to 1.10, is higher than the values previously reported, which are typically about 0.5. This may be due to the high jet Reynolds number range investigated in this work, as the jet Reynolds numbers reported in the previous works are considerably lower (from 4000 to 70,000). A

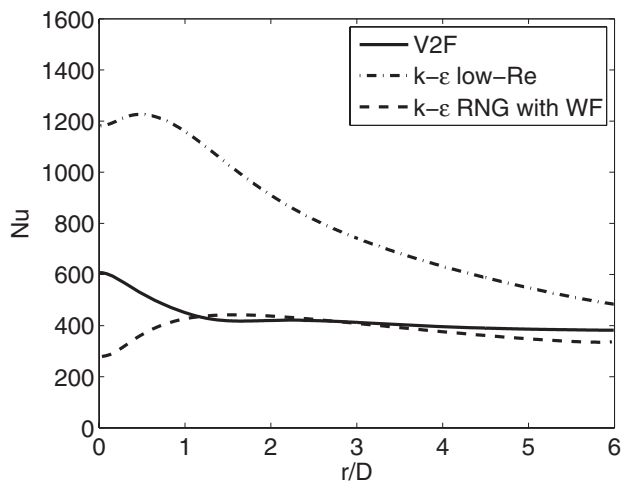


Figure 7 Nusselt number distributions obtained using different turbulence models.

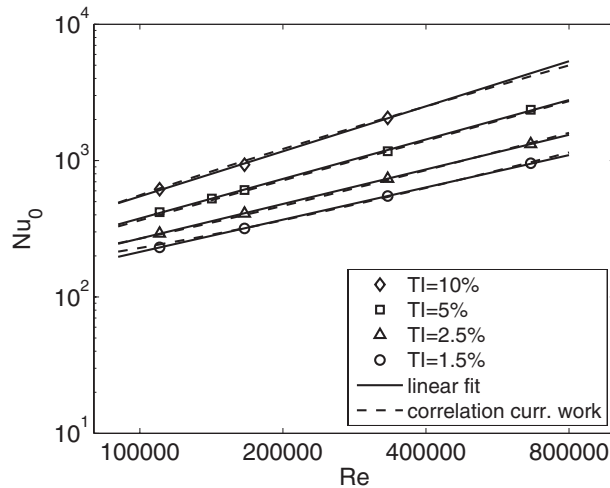


Figure 8 Stagnation point Nusselt number versus jet Reynolds number.

higher jet Reynolds number may result in the development of higher turbulence levels when approaching the stagnation point and therefore increased heat transfer. For a purely laminar jet flow, the exponent value has been reported to be 0.5 [20, 21]. Differences in the turbulence intensity at the jet inlet would also influence the stagnation point heat transfer. However, we did not find statements about the turbulence intensity at the jet inlet in the cited works.

The stagnation point Nusselt numbers are plotted against the turbulence intensities at the jet inlet in Figure 9 for the data points in Figure 8 at $Re = 1.10 \times 10^5$, 1.66×10^5 , 3.32×10^5 , and 6.64×10^5 in order to study the variation in stagnation point Nusselt number with the turbulence intensity at the jet inlet.

For a fixed jet Reynolds number, a linear relationship is observed between the stagnation point Nusselt number and the turbulence intensity at the jet inlet, which can be expressed as $Nu_0 = aTI + b$, where a and b are constants. However, for different jet Reynolds numbers, a and b vary. Therefore, a and b should be functions of the jet Reynolds number.

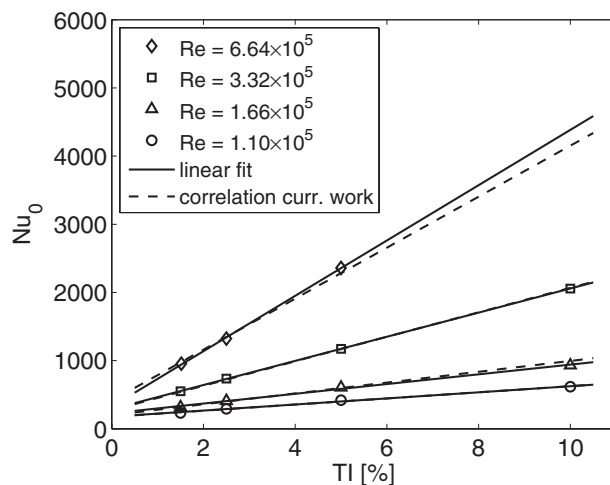


Figure 9 Stagnation point Nusselt number versus turbulence intensity at the jet inlet.

Based on the observed relationships between Nu_0 , Re and TI , a correlation is suggested of the form $Nu_0 = (c_1 TI + c_2) Re^\gamma + (c_3 TI + c_4)$, where c_1 , c_2 , c_3 , c_4 , and γ are constants. The correlation has been fit to the data points presented in Figures 8 and 9 to determine c_1 , c_2 , c_3 , c_4 , and γ . A least-squares method was applied to minimize the relative error between the stagnation point Nusselt numbers obtained from the simulations and those predicted by the correlation. The resulting correlation is:

$$Nu_0 = (0.103 TI + 7.41 \times 10^{-4}) Re^{0.96} - (2626 TI - 124) \quad (4)$$

The correlation is valid for jet Reynolds numbers from 1.10×10^5 to 6.64×10^5 and turbulence intensities at the jet inlet from 1.5% to 10%, given as $TI = 0.015$ to $TI = 0.10$ in Eq. (4). Within these limits, the maximum deviation between the stagnation point Nusselt numbers obtained from the simulations and the corresponding Nusselt numbers predicted by the correlation is 7%. Stagnation point Nusselt numbers obtained using the correlation are presented in Figures 8 and 9.

In a previous experimental work by den Ouden and Hoogendoorn [5], a correlation between Nu_0 , Re and TI was suggested of the form:

$$Nu_0 = (0.497 + 3.48 \times 10^{-2} (TI Re^{0.5}) - 3.99 \times 10^{-4} (TI Re^{0.5})^2) Re^{0.5} \quad (5)$$

The correlation is apparently valid for jet Reynolds numbers up to 2.64×10^5 , turbulence intensities at the jet inlet up to 7.25%, and H/D ratios below 4. However, the validity ranges were not clearly stated in reference [5]. Hofmann et al. [17] recently suggested a correlation for the local Nusselt number Nu in terms of Re , r/D , and the Prandtl number ($Pr = \mu c_p / \lambda$), but with no explicit description of the influence of the turbulence intensity at the jet inlet:

$$Nu = 0.055 (Re^3 + 10 Re^2)^{0.25} Pr^{0.42} \exp(-0.025 (r/D)^2) \quad (6)$$

The correlation of Hofmann et al. [17] was stated to be valid for jet Reynolds numbers between 1.40×10^4 and 2.30×10^5 , H/D ratios from 0.5 up to 10, and r/D ratios up to 8. Hence, the correlation in Eq. (6) is also valid in the stagnation point. No validity range was given for Pr . For comparison, the correlation suggested in the present work (Eq. (4)), the correlation by den Ouden and Hoogendoorn [5], and the correlation by Hofmann et al. [17] have been applied for the jet Reynolds numbers where their validity ranges overlap, that is, jet Reynolds numbers between 1.10×10^5 and 2.30×10^5 . The turbulence intensity was varied between 2.5% and 7.5%, and as the Prandtl number in all the performed simulations in the present work was 0.67, this value was applied for the correlation in Eq. (6). The resulting stagnation point Nusselt numbers are presented in Figure 10.

Stagnation point Nusselt number predictions obtained with the correlation suggested in the current work (Eq. (4)) are observed to lie above the predictions obtained with the correlation of den Ouden and Hoogendoorn [5] (Eq. (5)) for all three

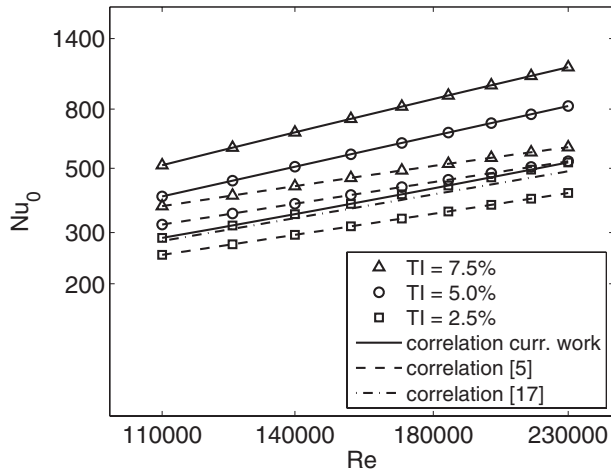


Figure 10 Stagnation point Nusselt number predictions by different correlations.

turbulence intensities in the investigated jet Reynolds number range (the average deviation is 43%). Predictions by the correlation of Hofmann et al. [17] are also found to be lower than those of the correlation in Eq. (4). Between $TI = 2.5\%$ and $TI = 5\%$ (typical intensity range for fully developed pipe flows), predictions by the suggested correlation in Eq. (4) are on average 31% higher than predictions by the correlation of Hofmann et al. [17]. These findings may indicate that the suggested correlation in the present work to some degree overpredicts the stagnation point Nusselt number. An overprediction by the numerical model in the stagnation region was also observed in the validation study. However, the correlations used for comparison are based on jet impingement heat transfer data obtained in configurations that differ from the configuration investigated in the present work. Considerably lower temperature differences and pressures were present in these configurations, and the jets were issuing from pipe nozzles with fully developed flow profiles, contrary to the investigated case in the present work. A proper evaluation of the suggested correlation in Eq. (4) needs to be performed against detailed experimental data for conditions similar to those in the investigated configuration.

Besides the investigated effects of Re and TI on the stagnation point Nusselt number, the dimensionless groups Pr and H/D also influence Nu_0 , but the influence of these groups was not studied in the present work.

CONCLUSIONS

Jet impingement heat transfer has been investigated numerically in a configuration with a high jet Reynolds number and a large temperature difference between jet inlet and wall. The configuration conditions were based on the conditions in a large marine diesel engine during combustion when hot combustion products impinge on the piston surface.

The turbulence intensity at the jet inlet was found to have a pronounced influence on the wall heat transfer, especially in

the stagnation region. Additionally, a linear relationship was observed between the Nusselt number in the stagnation point and the turbulence intensity at the jet inlet.

Application of three different turbulence models showed a large variation in both the magnitude and the distribution of the predicted wall heat transfer, especially in the stagnation region.

Furthermore, the variation of stagnation point heat transfer with jet Reynolds number and the turbulence intensity at the jet inlet was investigated, and a correlation has been suggested for impinging jet flow cases with a jet Reynolds number between 1.10×10^5 and 6.64×10^5 and a turbulence intensity at the jet inlet between 1.5% and 10%. Further experimental validation of the suggested correlation is needed, however, which requires detailed experimental data at high jet Reynolds numbers and a large temperature difference between jet inlet and wall.

NOMENCLATURE

c_1, c_2, c_3, c_4	constants in Nu_0 correlation (—)
c_p	specific heat capacity at constant pressure (J/kg-K)
D	jet inlet diameter (m)
H	distance between jet inlet and wall (m)
h	enthalpy (J/kg)
Nu	Nusselt number, $Nu = \alpha D / \lambda$ (—)
Nu_0	stagnation point Nusselt number (—)
p	pressure (Pa)
Pr	Prandtl number, $Pr = \mu c_p / \lambda$ (—)
q_w	wall heat flux (W/m^2)
r	radial distance from center axis (m)
Re	jet Reynolds number, $Re = \rho V D / \mu$ (—)
T_j	temperature at jet inlet (K)
T_w	wall temperature (K)
TI	turbulence intensity at jet inlet (—)
u_i	velocity component along the i th coordinate direction (m/s)
V	velocity at jet inlet (m/s)
x_i	i th Cartesian coordinate (m)
y	distance to the wall (m)
y^+	dimensionless wall distance, $y^+ = y \sqrt{\tau_w \rho} / \mu$ (—)

Greek Symbols

α	heat transfer coefficient (W/m^2-K)
γ	exponent in Nu_0 correlation (—)
δ_{ij}	the Kronecker delta (—)
λ	thermal conductivity ($W/m-K$)
μ	dynamic viscosity ($N-s/m^2$)
ρ	density (kg/m^3)
τ_{ij}	stress tensor (N/m^2)
τ_w	wall shear stress (N/m^2)

Superscripts

- time-averaged value
 / turbulent fluctuation

REFERENCES

- [1] Zuckerman, N., and Lior, N., Impingement Heat Transfer: Correlations and Numerical Modeling, *ASME Journal of Heat Transfer*, vol. 127, no. 5, pp. 544–552, 2005.
- [2] Martin, H., Heat and Mass Transfer Between Impinging Gas Jets and Solid Surfaces, *Advances in Heat Transfer*, vol. 13, pp. 1–60, 1977.
- [3] Viskanta, R., Heat Transfer to Impinging Isothermal Gas and Flame Jets, *Experimental Thermal and Fluid Science*, vol. 6, no. 2, pp. 111–134, 1993.
- [4] Shi, Y., Mujumdar, A. S., and Ray, M. B., Effect of Large Temperature Difference on Impingement Heat Transfer Under a Round Turbulent Jet, *International Communications in Heat Mass Transfer*, vol. 31, no. 2, pp. 251–260, 2004.
- [5] den Ouden, C., and Hoogendoorn, C. J., Local Convective Heat-Transfer Coefficients for Jets Impinging on a Plate: Experiments Using a Liquid-Crystal Technique, *Proceedings of 5th International Heat Transfer Conference*, pp. 293–297, 1974.
- [6] Baughn, J. W., and Shimizu, S., Heat Transfer Measurements From a Surface With Uniform Heat Flux and an Impinging Jet, *ASME Journal of Heat Transfer*, vol. 111, no. 4, pp. 1096–1098, 1989.
- [7] Behnia, M., Parneix, S., Shabany, Y., and Durbin, P. A., Numerical Study of Turbulent Heat Transfer in Confined and Unconfined Impinging Jets, *International Journal of Heat and Fluid Flow*, vol. 20, no. 1, pp. 1–9, 1999.
- [8] Hofmann, H. M., Kaiser, R., and Kind, M., Calculations of Steady and Pulsating Impinging Jets—An Assessment of 13 Widely Used Turbulence Models, *Numerical Heat Transfer, Part B*, vol. 51, no. 6, pp. 565–583, 2007.
- [9] Gordeev, S., Heinzl, V., and Slobodchuk, V., Simulation of Single and Multiple Impinging Jet Cooling and Comparison with Experimental Data, *Proceedings of 8th Biennial ASME Conference on Engineering Systems Design and Analysis, ESDA2006*, pp. 143–158, 2006.
- [10] Durbin, P. A., Near-Wall Turbulence Closure Modeling Without “Damping Functions,” *Theoretical and Computational Fluid Dynamics*, vol. 3, no. 1, pp. 1–13, 1991.
- [11] Behnia, M., Parneix, S., and Durbin, P. A., Prediction of Heat Transfer in an Axisymmetric Turbulent Jet Impinging on a Flat Plate, *International Journal of Heat and Mass Transfer*, vol. 41, no. 12, pp. 1845–1855, 1998.
- [12] Lien, F. S., Chen, W. L., and Leschziner, M. A., Low-Reynolds-Number Eddy-Viscosity Modelling Based on Non-Linear Stress-Strain/Vorticity Relations, *Proceedings of 3rd Symposium on Engineering Turbulence Modelling and Measurements*, 1996.
- [13] Yakhot, V., Orszag, S. A., Thangam, S., Gatski, T. B., and Speziale, C. G., Development of Turbulence Models for Shear Flows by a Double Expansion Technique, *Physics of Fluids A*, vol. 4, pp. 1510–1520, 1992.
- [14] Perry, R. H., Green, D. W., and Maloney, J. O., *Perry’s Chemical Engineers’ Handbook*, 6th ed., McGraw-Hill, Singapore, 1984.
- [15] CD-adapco, *Methodology, STAR-CD version 4.14*, 2010.
- [16] Launder, B. E., and Spalding, D. B., The Numerical Computation of Turbulent Flows, *Computer Methods in Applied Mechanics and Engineering*, vol. 3, no. 2, pp. 269–289, 1974.
- [17] Hofmann, H. M., Kind, M., and Martin, H., Measurements on Steady State Heat Transfer and Flow Structure and New Correlations for Heat and Mass Transfer in Submerged Impinging Jets, *International Journal of Heat and Mass Transfer*, vol. 50, no. 19–20, pp. 3957–3965, 2007.
- [18] Petzold, K., Der Wärmeübergang an einer senkrecht angeströmten Platte, *Wiss. Z. Techn. Univ. Dresden*, vol. 13, pp. 1157–1161, 1964.
- [19] Lee, D., Greif, R., Lee, S. J., and Lee, J. H., Heat Transfer From a Flat Plate to a Fully Developed Axisymmetric Impinging Jet, *ASME Journal of Heat Transfer*, vol. 117, no. 3, pp. 772–776, 1995.
- [20] Hollworth, B. R., and Gero, L. R., Entrainment Effects on Impingement Heat Transfer: Part II—Local Heat Transfer Measurements, *ASME Journal of Heat Transfer*, vol. 107, no. 4, pp. 910–915, 1985.
- [21] Hoogendoorn, C. J., The Effect of Turbulence on Heat Transfer at a Stagnation Point, *International Journal of Heat and Mass Transfer*, vol. 20, no. 12, pp. 1333–1338, 1977.



Michael V. Jensen is a Ph.D. student at the Department of Mechanical Engineering at the Technical University of Denmark. He received his M.Sc. degree in mechanical engineering in 2006 from the Technical University of Denmark. His research field is heat transfer in large two-stroke marine diesel engines.



Jens H. Walther is an associate professor in fluid mechanics at the Technical University of Denmark. He is also a research associate at the Chair of Computational Science at ETH Zurich, Switzerland. He received his Ph.D. degree in 1994 from the Technical University of Denmark. His main research interests are in numerical fluid dynamics and range from atomistic simulations of fluid flow at the nanoscale to large-scale simulations in bluff body aerodynamics.